# POLAR MOTION AND NON TIDAL SIGNALS IN THE SUPERCONDUCTING GRAVIMETER OBSERVATIONS IN BRUSSELS

**B. Ducarme [1)*], M. van Ruymbeke[1)], A.P. Venedikov [2,3)], J. Arnoso [2)], R. Vieira [2)]**

[1)] Royal Observatory of Belgium. Av. Circulaire, 3. B-1180 Bruxelles. Belgium ducarme@oma.be

[2)] Instituto de Astronomía y Geodesia (CSIC-UCM). Facultad de Matemáticas, Plaza de Ciencias, 3. 28040 Madrid. Spain. arnoso@iagmat1.mat.ucm.es, vieira@iagmat1.mat.ucm.es

[3)] Geophysical Institute, Bulgarian Academy of Sciences, Acad. G. Bonchev street, block 3, Sofia 1113. Bulgaria. vened@geophys.bas.bg

(*) **Corresponding author**:
TEL: +32 2 3730248
FAX: +32 2 3749822
E-MAIL: ducarme@oma.be

## ABSTRACT

Through the analysis of 13½ years of tidal gravity observations the gravity effect of the polar motion is estimated, that is, the amplitude factor $\delta_{pole}$ of the pole tide. This data set is extracted from the complete series of 18 years (from 21.04.1982 till 22.09.2000) tidal data obtained in Brussels (Royal Observatory of Belgium) with the GWR T003 Superconducting Gravimeter (SG), from which a non-reliable initial part has been discarded. Very important precondition of success of this work is that the length of 13½ years allows a good separation of the annual components of the data and the Chandler wobble. The analysis has been performed with the computer program VAV/2002 (Venedikov et al., 2001, 2003) for tidal data processing. Some options have been specially developed for this task. The analysis has taken into account the tidal signal, including a rather efficient determination of the LP (long period) tides, seldom well estimated, as well as the effect of the air-pressure. We build then a model of the non tidal part of the signal often called "drift", directly orientated towards the estimation of $\delta_{pole}$. We include the theoretical pole tide, estimated from the IERS observations, multiplied by $\delta_{pole}$, a piecewise polynomial representation, an annual components at 1cpy (cycle per year) with its harmonics till 6 cpy and a model of the temperature effect. The result obtained for the polar motion tidal factor is $\delta_{pole} = 1.181 \pm 0.008$. This is higher value than the value $\delta=1.158$ theoretically predicted for periods near one year by a model including mantle inelasticity. The difference is due to the tidal loading effect of the ocean pole tide. It appeared impossible to get a good estimate of $\delta_{pole}$ when the water table is included in the drift model due to a strong interference with the polynomials, approximating the instrumental drift. Nevertheless, the effect of the water table, i.e. the corresponding regression coefficient $c_{WT}$, has been separately estimated, so to say, as a

byproduct of the main task. The regression coefficient obtained for the water table $c_{WT} = -\quad \pm \quad$ $^{-2}$/m which is in reasonable agreement with previous determination.

## 1. INTRODUCTION

The Superconducting Gravimeter (SG) GWR model T003 recorded tidal variations of gravity at station Brussels, situated in the Royal Observatory of Belgium, from 21.04.1982 till 22.09.2000, i.e. some 18 years. This is the longest set of SG tidal data ever obtained.

In principle, SG instruments have a very low drift, especially in comparison to other tidal instruments, namely spring gravimeters, tiltmeters and extensometers. This makes the SG data very interesting with respect to the study of low frequency phenomena, in particular the gravity effect of the polar motion, the so-called "pole tide".

The pole tide is dominated by the 430-day Chandler wobble and an annual component. A major problem in studying the pole tide is that the tidal data also contain an annual component of meteorological origin, coinciding with the long period tide Sa (solar annual tide). This makes it necessary to separate the pole tide from the spurious annual contribution. Such a process needs records of at least 6.6 years, the longer – the better.

In July 1997 started (Crossley et al., 1999) Global Geodynamics Project (GGP) observation campaign. It involves stations with the new generation of SG, namely the Compact-Tidal (CT) instruments. The latter have better performances than the T model in Brussels. Nevertheless, due to the need for series larger than 6.6 years, the data of Brussels remain most promising with respect to the pole tide, as it covers several commensurability intervals between the Chandler and annual periods.

In the following parts of this paper we shall consider the study of the pole tide through specially developed analysis of the SG data of Brussels.

Section 2 introduces a general model of the gravity effect of the polar motion. In analogy with the long period tides, a polar amplitude $\delta$ factor is defined, which relates the theoretical pole tide with the observed one.

Section 3 is a brief description of the SG data from Brussels.

Sections 4 and 5 discuss with the method of analysis, which is applied by the computer program VAV for tidal data processing. In section 4 the drift is modeled as a stepwise function, remaining a constant during 24 hours. The values of the drift are included in the observational equations as unknowns, which are estimated by MLS (Method of the least squares). Further, in Section 5, the drift is represented as a combination of purely instrumental drift, observed pole tide, temperature effects, annual component and the effect of the water table.

In subsections 5.1 an initial part of the data is abandoned and the finding of an optimum initial point is shown. Subsections 5.2 through 5.6 deals with finding concrete components of the general drift function. The models involve series of parameters, whose values are not defined a priory. Some optimum values are found in a Bayesian approach, though variations of the models and selection of optimum variants on the basis of statistical criteria.

Most sophisticated and thus most vulnerable may look the polynomial model of the drift, discussed in subsection 5.2. In principal, polynomials are used as a most flexible tool for the approximation of non-periodical functions. Since the drift has obviously discontinuities, as jumps, and discontinuities in its derivates, manifested as sudden changes of the drift behavior, it was impossible to get a good approximation by a single model over the whole data interval of 13 years. Therefore the data series has been partitioned in 4 blocks and the drift has been approximated by different polynomials in every block. It is shown how the points of the discontinuities are found and how the power of the polynomials is chosen.

Subsections 5.3, 5.4 and 5.5 deal with the models of the annual, temperature and water table components. The last subsection 5.6 deals with the pole tide. Here a more general model is used

than the model in section 2. Namely, a possibility of a time lag between the theoretical and the observed pole tide is accepted. Nevertheless, the estimated time lag appeared to be insignificantly low (advance of 4 days).

The final results, actually obtained in section 5, are presented in section 6.

## 2. POLE TIDE AND LONG PERIOD TIDAL COMPONENTS

Let $\Delta g(T)$ is the theoretical tidal gravity signal at given place and time $T$, generated by the tide generating potential of degree 2. This means that $\Delta g(T)$ is a variation of the gravity which would be observed on an ideal non-deformable (absolute rigid) Earth.

According to the classical theory of Love, in the case of static deformation of the Earth, the observed tidal gravity variations are

$$\Delta G(T) = \delta\, g(T) \qquad (1)$$

I.e., due to the deformation, $\Delta g(T)$ is multiplied by a coefficient, often called delta or amplitude factor.

In the actual case, the picture is not so simple. The expression (1) is considered in the frequency domain with a frequency dependent $\delta$ factors and it is necessary to introduce phase lags, which are also frequency dependent.

Nevertheless, for the tidal constituents with very low frequencies or the LP (long period) tides, especially those at frequencies 1 cpy (cycle per year) the expression (1) works quite well. There are at least three reasons for this: (i) the deformation is very slow, (ii) the amplitudes of the ocean tides, whose loading effect may affect (1), have very small amplitudes and (iii) generally, the precision of all estimations at the low frequencies is very low and small deviations from (1) cannot be distinguished, being under the level of the noise.

Due to the polar motion the geographic latitude of a given point (a tidal station, for instance) and thus its distance to the Earth rotation axis are varying. This is changing the centrifugal force associated to the angular speed of the Earth rotation $\Omega$. Moreover, the variations of the length of the day, LOD(t) produce additional inertial forces modifying the gravity value.

By using the instantaneous pole coordinates $x(t), y(t)$ at time $t$ in arc seconds and the variation of the length of the day $dt$ in seconds per day, the theoretical change of gravity $\Delta$ (Melchior, 1986) at point with geographic coordinates $(\varphi,\lambda)$ can be computed through

$$\Delta = \Omega + + 0)dt \qquad (2)$$

where $r$ is the geocentric radius.

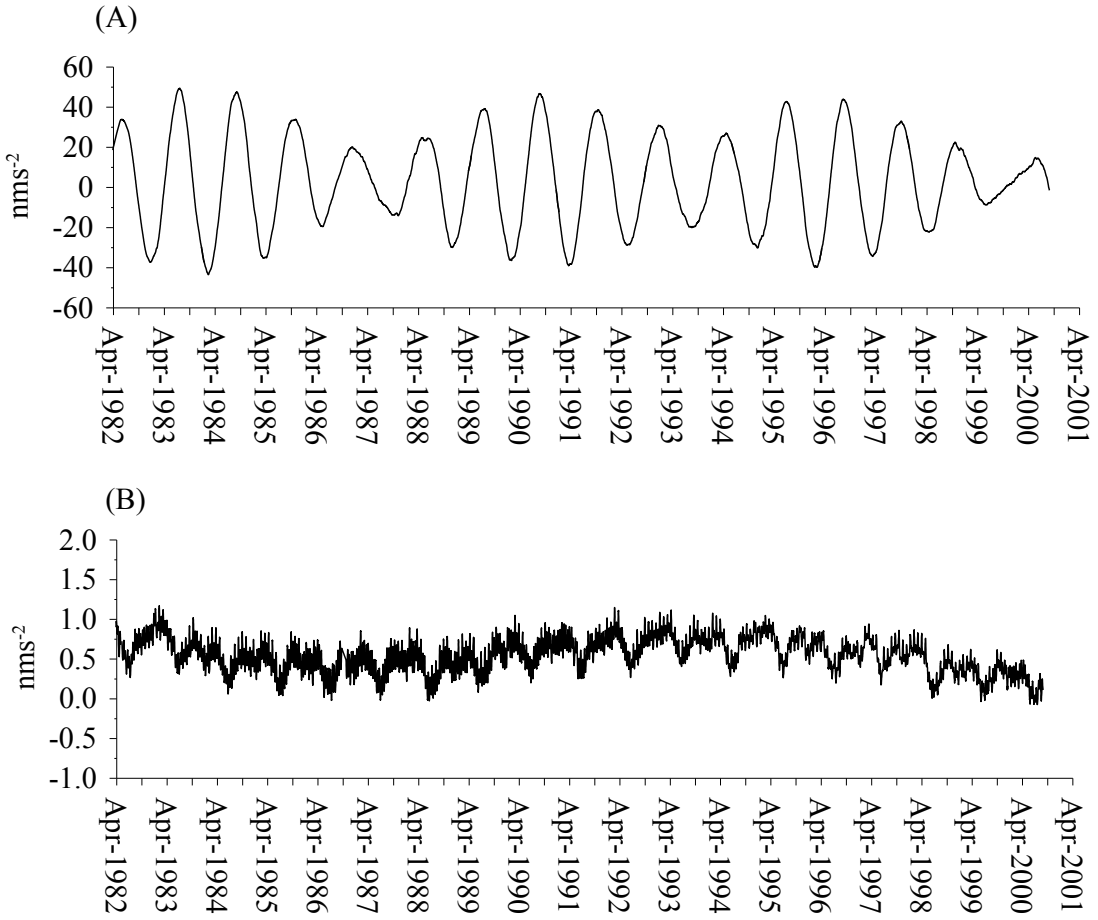


**Figure 1.** (**A**) The first term in (2) of the theoretical pole tide $\Delta$ for station Brussels. (**B**) The second term in (2) of the theoretical pole tide $\Delta$ for station Brussels.

Figures 1A and 1B represent the two components of $\Delta$ at station Brussels. The first one is, so to say, the theoretical effect of the proper polar motion, while the second one is the effect of LOD. Obviously, the effect of LOD is considerably lower, practically negligible.

The effect (2) can be called "theoretical" because it is computed for an ideal no deformable Earth, just like the theoretical tide $\Delta g(T)$ in (1). At the same time the polar motion causes a deformation of the real Earth, which has an effect on the gravity variations. Thus, instead of the theoretical pole tide $\Delta$ we shall observe a modulated pole tide $\Delta$ .

Nearly all LP tides are generated by the spherical harmonic of the tide generating potential of degree 2, order 0 (zonal). The polar motion is also producing a potential field of degree 2, order 0 (zonal), the LP tides. Hence, the pole tide is amplified by the elastic response of the Earth in a similar way as the LP tidal waves. I.e., in analogy with (1), we can define an amplitude factor $\delta_{pole}$ through the relation

$$\Delta \quad = \quad \Delta \qquad (3)$$

This definition is in accordance with Dehant et al. (1999) for the $\delta$ factor (called tidal gravimetric factor): *"In the frequency domain, the tidal gravimetric factor is the transfer function between the tidal force exerted along the perpendicular to the ellipsoid and the tidal gravity changes along the vertical as measured by a gravimeter".*

For a purely elastic Earth, Dehant et al. (1999) computed a latitude dependent $\delta$ value, which for Brussels (50°48') was $\delta = 1.15534$. Inelasticity in the mantle increases the $\delta$ value for longer periods (Table 1).

The usual methods for tidal analysis are not able to provide valuable determination of LP tides like the annual Sa wave or its harmonic the semiannual Ssa, as they are always strongly affected by meteorological effects. Therefore, our unique possibility to investigate the Earth deformation at very low frequencies and thus to check the theoretical values in Table 1 is to try to determine the amplitude factor $\delta_{pole}$ of the pole tide.

**Table 1** Tidal gravity factors for the long period waves. Model DDW99, inelastic, non hydrostatic.

| Wave | Angular speed (°/h) | Period (days) | Amplitude Factor $\delta$ |
|---|---|---|---|
| MQm | 2.18678245 | 6.86 | 1.15598 |
| MsQm | 2.11392880 | 7.10 | 1.15599 |
| MTm | 1.64240775 | 9.13 | 1.15608 |
| MsTm | 1.56955409 | 9.56 | 1.15609 |
| Mf | 1.09803304 | 13.66 | 1.15622 |
| Msf | 1.01589576 | 14.77 | 1.15625 |
| Mm | 0.54437471 | 27.55 | 1.15649 |
| Msm | 0.47152105 | 31.81 | 1.15655 |
| Ssa | 0.08213728 | 186.62 | 1.15738 |
| Sa | 0.04106668 | 365.26 | 1.15778 |
| 18 years | 0.00220641 | 7267.09 | 1.15996 |

As shown by Figure 2, the Chandler wobble is clearly distinguished in both the gravity data and the theoretical pole tide. This is an indication, that the gravity data can be used to study the pole tide. An annual component with 1 cpy also exists in both types of data, but the annual gravity component is much stronger and it is accompanied by a sub-harmonic of 2 cpy. Strong energy can also be seen in the gravity spectrum at frequencies lower than 0.5 cpy which are actually related with the drift.

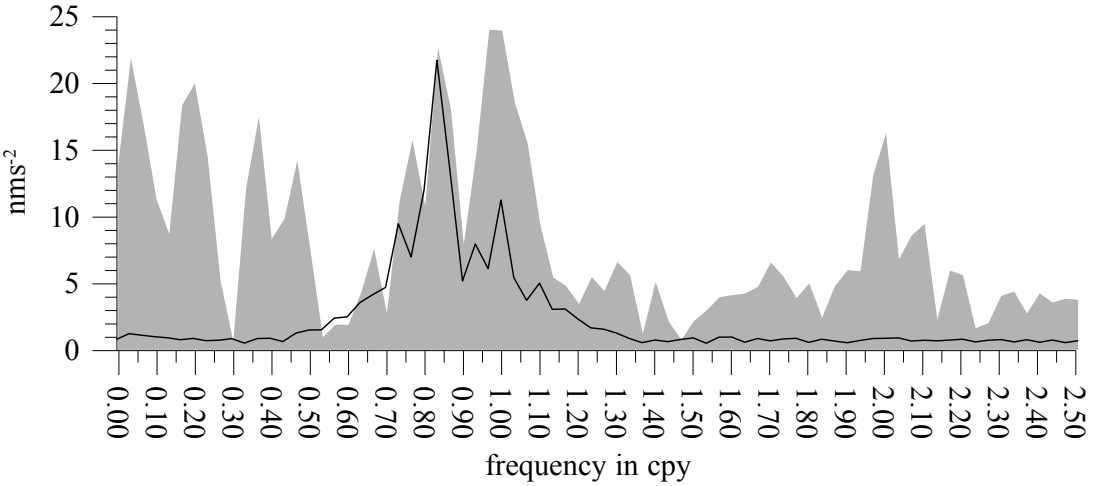


**Figure 2.** Very long period spectrum of the observed gravity signal (filled curve) and the theoretical pole tide. showing the complex structure around 1 cpy (cycles per year) and the Chandler period (0.85 cpy). The superimposed spectrum of the polar motion indicates that the Chandler term is very well recorded but that the annual one is largely contaminated. There is also significant energy in periods larger than 750 days (frequencies lower than 0.5 cpy) that we try to model by a piecewise polynomial representation.

## 3. THE SUPERCONDUCTING GRAVITY DATA IN BRUSSELS

As said above, the superconducting gravimeter T003 recorded at the Royal Observatory of Belgium between 21.04.1982 and 22.09.2000. The series is split in two main parts.

A first period extending from April 1982 to October 1986 has been extensively studied in De Meyer and Ducarme (1991). The long term behavior of the instrument was seriously disturbed until May 1986 by the so called “getter” effect. As there was a slight leak of helium gas in the vacuum can separating the core of the instrument from the liquid helium bath, the heating voltage of the thermostat had to increase steadily to compensate the increasing loss of energy by convection of the helium gas. After 6 months the maximum possible heating power has been reached and thus it became necessary to insert a “getter”, that is, a small porous ceramic crystal able to fix the helium gas. The voltage has then decreased to its minimum in one hour and a new cycle started. The voltage drop was accompanied by a jump in the gravimeter curve of the order of 3µgal/V (1µgal = $10^{-8}$ $ms^{-2}$ = 10 $nms^{-2}$) and followed by a slow upward drift during 6 months. The net result was to introduce an artificial 6 months periodicity in the data obscuring the annual term and the polar motion signal.

Since May 1986 (day 1500 in Figure 3) a permanent getter has been installed in order to solve that problem. However, the characteristics of the annual term as well as of the thermal effects concentrated in the $S_1$ term (frequency $\nu(S_1) =$ ) were modified. For example the annual term, evaluated to 30 $nms^{-2}$ in De Meyer and Ducarme (1991), increased up to 60$nms^{-2}$ after the introduction of the permanent "getter". It is thus difficult to study simultaneously the data obtained before and after May 1986. Moreover, an instrumental failure occurred in October 1986 and the ball had to be relevitated.

The second recording period, extending from November 1986 up to September 2000, is homogeneous and quite undisturbed, except at the beginning. After relevitation of the ball a strong drift occurred and a final adjustment of the parameters was performed in the spring of 1987. In section 5.1 we shall investigate the best initial epoch from a statistical point of view. We have found namely that it is in April 1987. This is the reason why we shall consider hereafter the data between April 1987 and September 2000 (13½ years) only.

## 4. DETERMINATION OF THE DRIFT IN SG DATA

The basic algorithm of VAV is related with the following model of the drift.

The data set is partitioned into a sequence of time intervals or blocks of equal length. We shall denote by $I(T)$ an interval with central epoch $T$. In an earlier computation we used intervals of length $L = 48^{\mathrm{h}}$. Now we have used $L = 24^{\mathrm{h}}$ with better results.

The intervals are without overlapping. Between the intervals may remain arbitrary gaps, as well as strongly perturbed and doubtful data. We have thus a set of intervals

$$I(T) \text{ with central epochs } T = T_1, T_2, T_3, \ldots \text{ where } T_{i+1} - T_i \geq L = 24 \text{ hours.} \qquad (4)$$

Let $Y(T+t)$ be an ordinate or tidal observation at time $T+t$ within $I(T)$, where $t$ is time, measured within $I(T)$ with origin $t = 0$ at the central epoch $T$. According to our model the drift $D(T+t)$ at the point $T+t$ is represented by the polynomial

$$D(T+t) = \sum_{l=0}^{k} d_l(T)\, t^l \text{ in a given } I(T). \qquad (5)$$

Here $d_l(T)$ are $k+1$ unknown constants in a given $I(T)$. In the same time $d_l(T)$ may get arbitrarily different values in the different $I(T)$, i.e. $d_l(T)$ are functions of the epoch $T$. It is very essential that $d_0(T) = D(T)$ is the value of the drift (according to the model) at the central epoch $T$.

We shall use the following general model or observational equations

$$Y(T+t) = G_{\mathrm{D,SD}}(T+t) + G_{\mathrm{LP}}(T+t) + G_{\mathrm{AP}}(T+t) + D(T+t),\ T = T_1, T_2, T_3, \ldots \qquad (6)$$

The *G* terms are components of the tidal record, different from the drift, namely

$G_{\mathrm{D,SD}}(T+t)$ is the usually treated tidal signal at the D, SD, … frequencies
$G_{LP}(T+t)$ is the long period (LP) tidal signal
$G_{\mathrm{AP}}(T+t)$ is the effect of the air-pressure and, eventually, other meteorological signals.

In this way the drift term $D$ can be considered as the unexplained long-term part of the signal.

Every one of the components in (6) involves a set of unknowns. The **statistically correct** processing of the data by using MLS (Method of the Least Squares) is to solve this system of equations **with all unknowns**, including the drift unknowns $d_k(T)$. According to this principle VAV provides MLS estimates $\widetilde{d}_l(T)$ of $d_l(T)$ and thus the estimated values $\widetilde{D}(T+t)$ of the drift, in particular the estimated drift $\widetilde{D}(T) = \widetilde{d}_0(T)$ at the central epochs $T = T_1, T_2, T_3, \ldots$ .

The tidal analyses methods, when we are not interested in the LP tides, usually ignore the term $G_{\mathrm{LP}}$, the LP being well approximated and represented by the drift polynomials or filtered out as in ETERNA.

We have worked in another way. We have established for the SG data that in short intervals, e.g. during 24 hours, the drift properly said, i.e. without the LP tides, is practically a constant.

I.e., if the LP term is kept in (6), it is possible to consider the drift in $I(T)$ as a constant, choose the power $k = 1$ in (5) and thus replace $D(T+\ ) = l_0(T)$. In such a way the drift is represented by a stepwise function, remaining a constant with a step of 24 hours.

This allowed us to use (6) as

$$Y(T+\ ) = \gamma_{\mathrm{D,SD}}(T+\ ) + \gamma_{\mathrm{LP}}(T+\ ) + \gamma_{\mathrm{AP}}(T+\ ) + l_0(T) \qquad (7)$$

Then the drift is obtained as a series of estimates of the unknowns $d_0(T)$ for $T = T_1, T_2, T_3, \ldots$ Figure 3 represents the drift curve obtained in such a way.

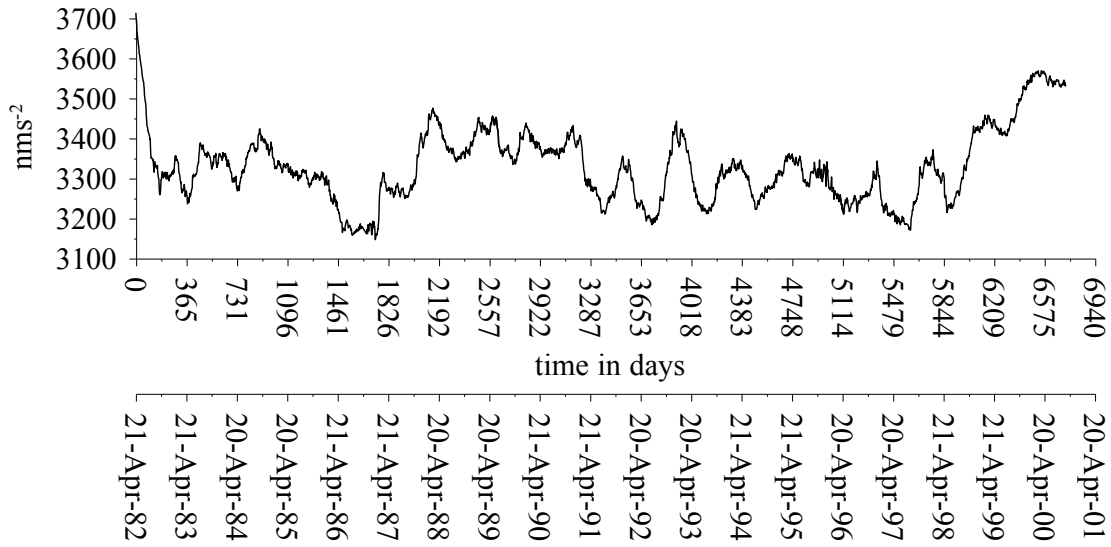


**Figure 3**. Complete curve of the estimated drift over the time interval of 18.4 years, from 21.04.1982 till 22.09.2000 and points every 24 hours (with the exception of two small gaps).

The model of the drift as a stepwise function, used here, also has been used for the determination of the LP tides (Ducarme et al., 2004 (Journal of Geodynamics, in press)). The results obtained, according to our knowledge, are with the highest precision ever reached, which confirms the reasonability of this model.

The solution of the system (7) by VAV, according to MLS, passes through a transformation of the data in a time/frequency domain. For every $I(T)$ we get a set of quantities, obtained by the application of orthogonal pass-band filters amplifying bands at frequencies 1, 2, … cpd, and low-pass filtered quantities, related with the estimation of $d_0(T) = \Im(T)$.

The tidal data are charged by a red noise. This is the reason VAV uses frequency dependent filtered data. Through their residuals we get frequency dependent estimates of the precision, always lower at the lower frequencies. The estimates of the precision of $d_0(T)$ and all quantities, related with $d_0(T)$, are obtained through the residuals of the low-pass filtered quantities, having the most unfavorable effect of the noise. I.e., the precision of $d_0(T)$ is estimated in the most severe way.

Partitioning in blocks of $L = 24$ hours has been used by Doodson (1928, 1941) for the analysis of ocean data, as well as by Pertsev (1958???). Lecolazet (1958) has used blocks with $L = 13$. The method of Venedikov (1966) has used $L = 18$ which have been implemented in the first successful application of MLS.

The determination of LP by the programs ETERNA and ANALYSE of Wenzel () uses a partitioning of the data in blocks, considerably longer than our intervals $I(T)$. Within the blocks the drift is approximated by polynomials with different coefficients in the different blocks. Gaps and jumps are available between the blocks. The VAV model (7) can be considered as a particular case of the scheme of Wenzel, namely when the blocks are of fixed length of 24 hours and the power of the polynomials is the lowest possible, i.e. $k =$ ).

## 5. MODEL OF THE DRIFT AS NON-TIDAL COMPONENT OF THE DATA

Further the drift curve in Figure 3 will be considered as non-tidal component of the data, involving an "instrumental drift" properly said, as well as signals, in which we shall be mainly interested. Thus we shall use a model like

$$d_0(T) = \text{ID}(T) + \Delta G_{\text{annual}}(T) + \Delta G_{\text{temper}}(T) + \Delta G_{\text{WT}}(T) + \Delta G_{\text{pole}}(T),\ T = \text{1}, T_2, T_3, \ldots (8)$$

The $\Delta G$ components are known geophysical signals, namely

$\Delta G_{\text{annual}}$ - annual component, mainly of meteorological origin
$\Delta G_{\text{temper}}$ - effect of the slow temperature variations
$\Delta G_{\text{WT}}$ - effect of the water table and, finally,
$\Delta G_{\text{pole}}$ - observed gravity variations due to the polar motion (wobble) .

The component $D_{\text{ID}}$ denotes the instrumental drift can also be considered as representing the zero line of the record. It is not excluded $D_{\text{ID}}$ to include some geophysical signals, which we do not know. A typical characteristic of $D_{\text{ID}}$ is that there are not obvious periodic components.

As shown in the following, the expression (8) can be considered as a regression with unknown regression coefficients. E.g. the $\delta_{\text{pole}}$ in $\Delta G_{\text{pole}}$, defined by (3) is such a regression coefficients. Hence, (8) can be treated by MLS as a system of observational regression equations. Actually, VAV proposes a more strict application of MLS. Namely, $d_0(T)$ from (8) is replaced in (7). Then MLS is applied on the new (7), providing estimates of all unknowns, including the regression coefficients of (8).

In the following parts of this section the models of all components of (8) are discussed. The models depend on parameters, which are not a priori defined and which cannot be estimated by MLS as unknowns. This imposes to use a kind of Bayesian approach, namely to let vary the parameters and choose optimum cases according to a reasonable criterion.

The main criterion used is the minimum of the MSD (mean standard deviation) of $\delta_{\text{pole}}$, denoted as $\sigma(\delta_{\text{pole}})$. The Akaike Information Criterion AIC (Sakamoto et al., 1986), based on the principle of the maximum likelihood, has also been taken into account.

In the set of components we have a number of parameters and models, which may be denoted as $A, B, C, D, \ldots$ Let their optimum variant is $A_{\text{opt}}, B_{\text{opt}}, C_{\text{opt}}, D_{\text{opt}}, \ldots$ This variant has been obtained "manually", through many hundreds of analyses. For instance, we let vary $A$ for some fixed $B, C, D, \ldots$ until we find a promising variant of $A'_{\text{opt}}$. Then we fix $A =$ … and let vary $B$ until we find a promising variant $B =$ . Afterwards we return to $A$ looking for new optimum at condition $B =$ , etc.

In the examples hereafter, if we discuss the variation of, say $A$, this is done at the condition of already found $B_{\text{opt}}, C_{\text{opt}}, D_{\text{opt}}, \ldots$ Thus the examples demonstrate only the final stage of the optimization procedure.

The attempts to give "equal rights" to $\Delta G_{\text{WT}}$ with all components in (8), have failed. The reason is that there is the interference between $\Delta G_{\text{WT}}$ and the polynomials, representing $D_{\text{ID}}$. Therefore our final results were obtained without $\Delta G_{\text{WT}}$. As compensation, $\Delta G_{\text{WT}}$ is separately studied in section 5.5.

It is logically expected (8) to include the air-pressure, but all attempts to do this appeared to be useless. The reason is that the spectrum of the air-pressure does not include clear annual or other low frequency components.

### 5.1. Starting point of the data.

According to the events, discussed earlier in section 3, a portion of the initial data is not convenient for our purposes. So that the first problem we had to solve is to determine how many of the initial data must be discarded.

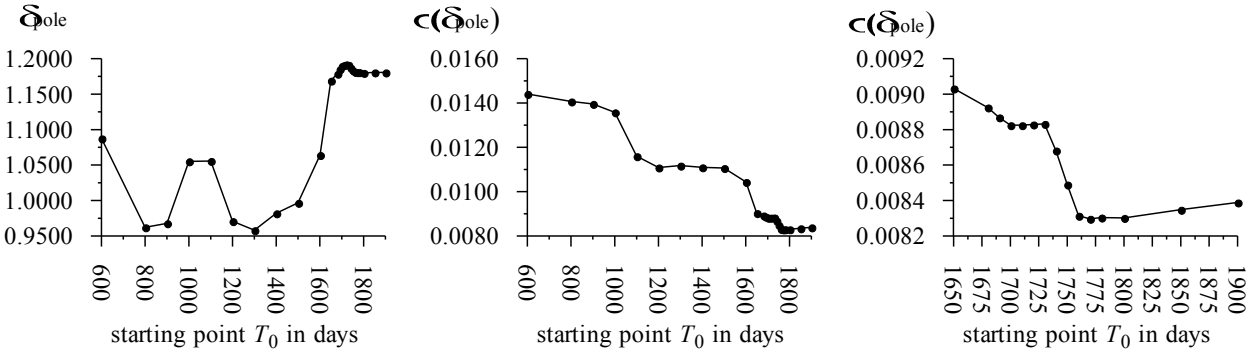


**Figure 4**. The factor $\delta_{\text{pole}}$ and its mean square deviation (MSD) $\sigma(\delta_{\text{pole}})$ as functions of the starting point $T_0$.

We have applied the analyses with different starting points $T_0$ between $400^{\text{d}}$ and $1900^{\text{d}}$. As shown in Figure 13, we have got a minimum of $\sigma(\delta_{\text{pole}})$ at $T_0 =$ , which has been accepted as a start of the data to be used.

### 5.2. Polynomial components, approximating the instrumental drift.

Generally, a universal tool for the approximation of an unknown function like $D_{\text{ID}}(T)$, which has not evident periodic components, is a polynomial of $T$ with appropriately chosen power $k$ and unknown coefficients (polynomial regression). In particular cases exponential functions can be useful (Richter et al., 1995, Loyer et al., 1999). Namely, the drift may have an exponential character during a certain time after its installation. Such is the initial part of Figure 3, which, by the way, has been discarded in section 5.1. Due to the complicated behavior of the data we preferred the polynomial approximation.

An intuitive study of Figure 3 clearly shows that there are several important changes in the tendencies of the curve, as well as some fast displacements, looking like jumps. Hence $D_{\text{ID}}(T)$ has to be considered as a discontinuous function at the jumps or as a continuous function with

discontinuous derivatives at some time points. Hence, it is senseless to use an approximation by a single polynomial, as well as by an exponential function, efficient only for continuous functions with continuous derivatives.

Due to this, we have decided to partition the curve in several segments or blocks and represent $D_{\mathrm{ID}}(T)$ by different polynomials in every segment. I.e., we accept that there are some discontinuities, which should separate the segments. In a way this is an approximation of the drift similar to its approximation in the blocks of Wenzel (see Section 4).

The search of the discontinuities has started by the partitioning of the data in two segments, separated by a variable point $T_{\mathrm{break}}$ (breaking point). Within every segment $D_{\mathrm{ID}}(T)$ has been represented by a polynomial of power $k =$ . We have let vary $T_{\mathrm{break}}$ from 2400 till 6400 days. The main results from these analyses are shown in Figure FNN_Tbreak_01. The relative minimums indicate possible discontinuities at about $T_{\mathrm{break}} = 3200^{\mathrm{d}}$ and, more clearly, at about $T_{\mathrm{break}} = 3700^{\mathrm{d}}$. Refining the search algorithm allowed to better localize these two points and to identify a third break point at about $T_{\mathrm{break}} = 4000^{\mathrm{d}}$.

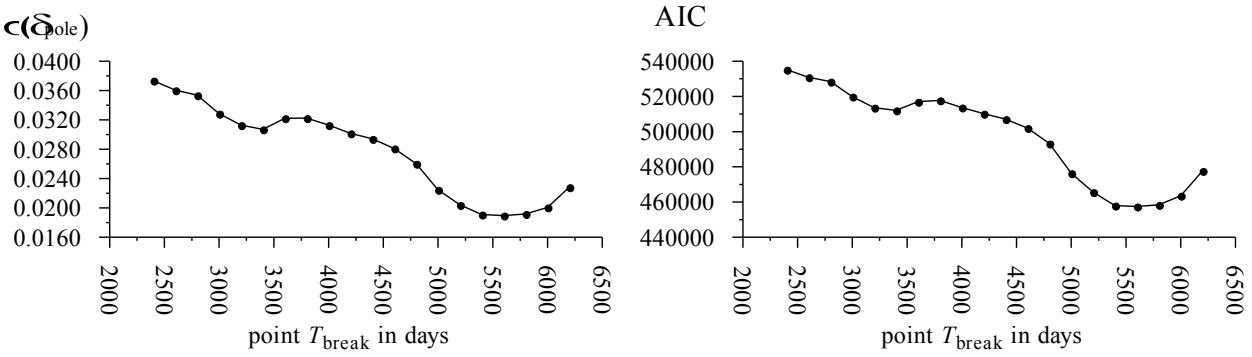


**Figure 5.** Experimental analyses for finding points of discontinuities of the instrumental drift.

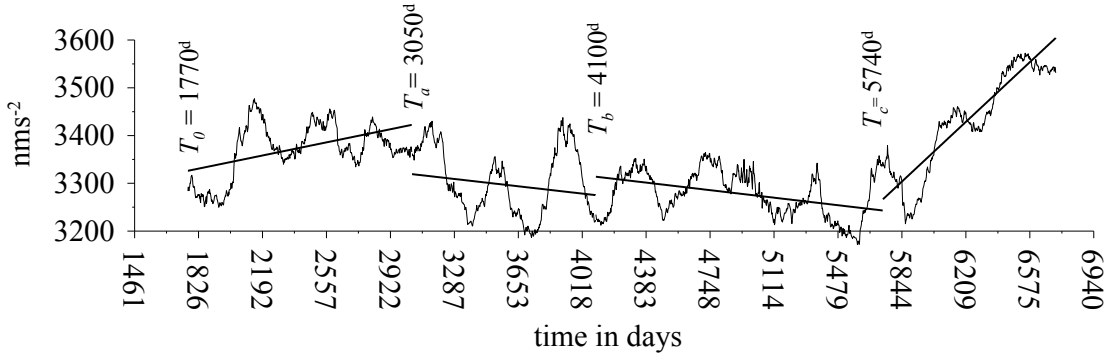


**Figure 6.** Points $T_a$, $T_b$ and $T_c$ of discontinuities, which define the partitioning of the data set in 4 segments.

Figure 6 shows the final selection of the discontinuity points and segments. The $D_{\mathrm{ID}}$ is approximated by linear functions with the only aim to illustrate the real changes in the character of the drift from segment to segment. Break points $T_a$ (day 3050) and $T_c$ (day 5740) correspond to a change of the slope of the instrumental drift and break point $T_b$ (day 4100) - to a jump.

The points $T_a, T_b$ and $T_c$ have been found after multiple experiments, looking for the minimum of $\sigma(\delta_{pole})$ and AIC. Figure 7 is an example of the final selection of the third point $T =$ . It is related to an abrupt change in the behavior of $D_{ID}(T)$ due to building activities at the Observatory including large excavations. They started in September 1997, at about $T =$ but it is impossible to know a priori when started the real effect of the building. The minimum has been found at $T_c =$ , some 100 days later than $T =$ .

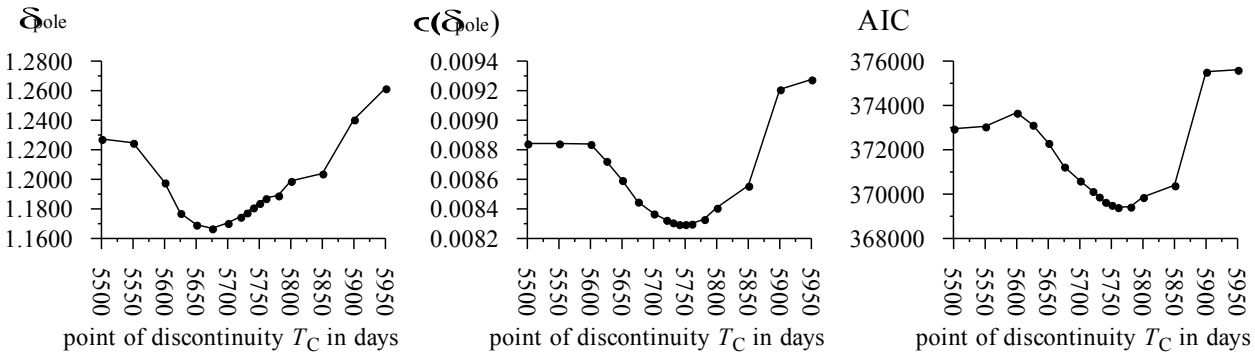


**Figure 7.** Estimated $\delta_{pole}$, MSD of $\sigma(\delta_{pole})$ and the criterion of Akaike AIC as functions of the point $T =$ of discontinuity.

Figure 8 shows the selection of the power $k$ of the polynomials, which is common to all the segments. It appeared to be an easy problem because we have got a clear minimum of $\sigma(\delta_{pole})$ for $k =$ . It is interesting that the curve of AIC does not stop decreasing at $k =$ . Nevertheless, due to the principle of parsimony, we have chosen $k =$ on the basis of $\sigma(\delta_{pole})$ .

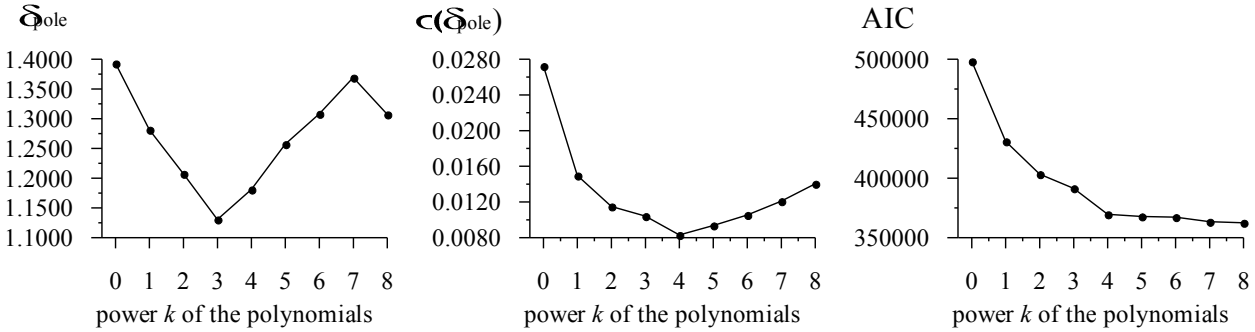


**Figure 8.** Estimated $\delta_{pole}$, its MSD $\sigma(\delta_{pole})$ and AIC as functions of the power $k$ of the polynomials in every segment.

### 5.3. Annual component.

It is very natural to represent $\Delta G_{annual}$ by a discrete Fourier expansion with basic period one year, namely

$$\Delta G_{annual}(T) = \sum_{j=1}^{J} h_j \cos\left(\frac{2\pi j}{a} T + \Phi_j\right), \text{ where } a = \text{ year in days and } T \text{ is also in days.} \qquad 9)$$

Here $h_j$ is amplitude and $\Phi_j$ is phase at frequency $j$ cpy. The regression unknowns are $h_j \cos\Phi_j$ and $h_j \sin\Phi_j$. The parameter of the model to be chosen is the order $J$.

The curves in Figure 9 have been obtained through analyses with different values of $J$. We haven't got a minimum of $\sigma(\delta_{pole})$, as well as of AIC. With good enough imagination, an effect can be seen till $J = 8$, but we have decided not to exaggerate and choose a final value $J = 5$, by keeping in mind the mentioned principle of parsimony. Moreover $\delta_{pole}$ becomes stable after $J = 5$ and $\sigma(\delta_{pole})$ as well as AIC are no more decreasing significantly.

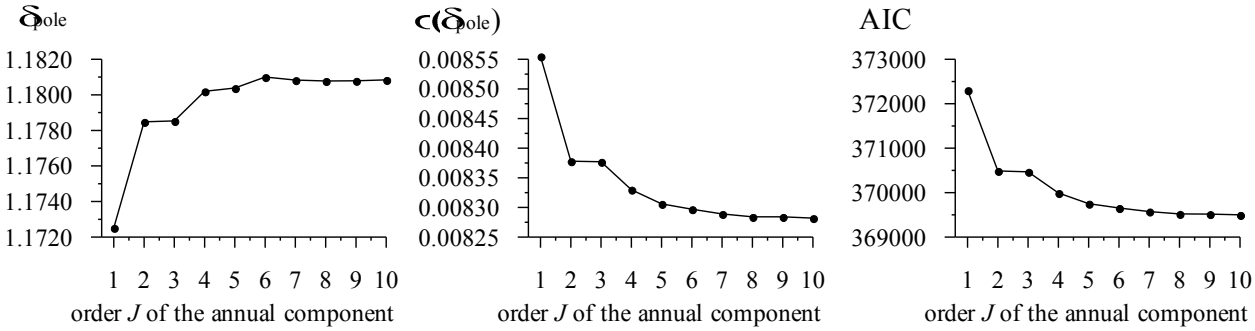


**Figure 9.** Estimated $\delta_{pole}$, its MSD $\sigma(\delta_{pole})$ and AIC as functions of the order (highest frequency) $J$ of the annual component.

As shown in the next section, the attempts to work without the annual component are to be categorically rejected.

### 5.4. Temperature component.

The effect of the temperature has been represented through

$$\Delta G_{temper}(T) = c_{temper}(C(T - \tau_{temper}) - \bar{C}), \qquad (10)$$

where $C(T)$ is mean daily temperature in $^{o}$C (degrees Celsius) at time $T$, $\bar{C}$ is mean of all used values of $C(T)$, $c_{temper}$ is an unknown regression coefficient and $\tau_{temper}$ is a time lag (retardation for $\tau_{temper} > 0$) of the effect of the temperature.

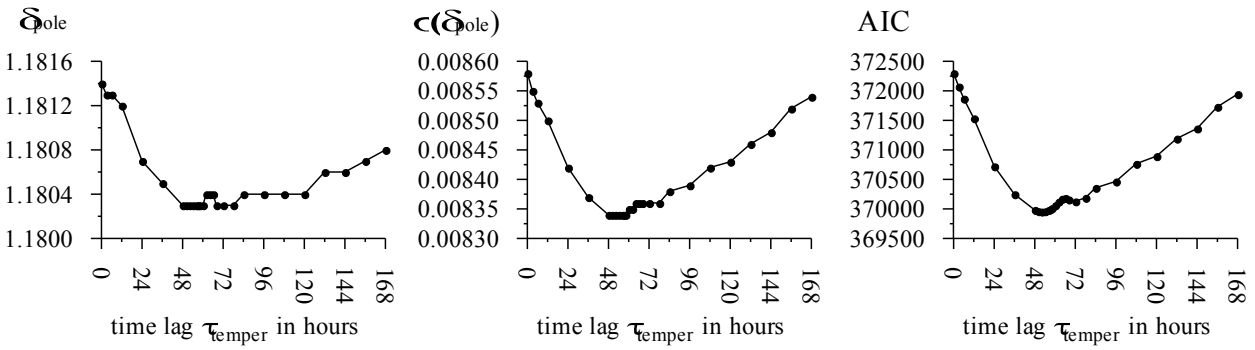

**Figure 10.** Estimated $\delta_{pole}$, its MSD $\sigma(\delta_{pole})$ and AIC as functions of the time lag $\tau_{temper}$ (retardation) of the temperature effect on the observed gravity.

The time lag $\tau_{temper}$ is a parameter of the model whose value has to be obtained through a variation procedure. As shown in Figure a minimum of $\sigma(\delta_{pole})$ at $\tau_{temper} =$ 52 hours. The minimum of AIC happened to be nearly at the same point.

**Table 2**. The effect of the temperature and the annual components.

| Case | Components used | | Regression coefficients | | Amplitudes $\Delta G_{annual}$ (nms$^{-2}$) | | |
|---|---|---|---|---|---|---|---|
| | $\Delta G_{temper}$ | $\Delta G_{annual}$ | $\delta_{pole}$ | $c_{temper}$ (nms$^{-2}$/K) | At 1 cpy | at 2 cpy | AIC |
| 1 | Yes | Not | 0.9608 ±0.0115 | -5.142 ±0.0385 | | | 403 383 |
| 2 | Not | Yes | 1.1839 ±0.0088 | | 53.21 ±0.26 | 6.52 ±0.26 | 375 007 |
| 3 | Yes | Yes | 1.1810 ±0.0083 | -1.735 ±0.047 | 40.72 ±0.37 | 5.22 ±0.24 | 369 653 |

Since the temperature has a seasonal annual component, it is interesting to investigate whether $\Delta G_{temper}$ cannot replace $\Delta G_{annual}$ and, vice-versa, whether $\Delta G_{annual}$ cannot replace $\Delta G_{temper}$. The results from these attempts are given in Table 2.

The case 1 without $\Delta G_{annual}$ is obviously very poor, compared to cases 2 and 3 with $\Delta G_{annual}$, i.e. $\Delta G_{annual}$ is absolutely necessary.

In case 1 we have $c_{temper}$ considerably higher (in absolute value) than in case 3. Thus $\Delta G_{temper}$ is partly taking the role of $\Delta G_{annual}$ but not enough. It is probably due to the fact that the semi-annual component is very weak in the temperature, in contradiction with what is observed in the gravity signal. A separate evaluation of both terms gives thus better results.

The comparison between cases 2 and 3 shows that $\Delta G_{temper}$ has a small, but useful effect on $\delta_{pole}$. It is also evident that the inclusion of $\Delta G_{temper}$ decreases the amplitude of $\Delta G_{annual}$. It can be explained by the fact that the amplitude of the annual wave in our residues is not perfectly stable as it is also the case for the annual temperature variations. The variable part of the annual gravity signal is effectively taken into account by the annual temperature wave, while the semi annual is not affected.

### 5.5. Effect of the water table

Figure 11 shows the observed curve of the water table $W(T)$ in Brussels. Following the experience of (Richter et al., 1995) and (Delcout-Honorez, 1991) we have accepted that the effect of $W(T)$ can be modeled by

$$\Delta G_{WT}(T) = \gamma_{WT} \left( W(T) - \bar{W} \right) \qquad (11)$$

where $c_{\mathrm{WT}}$ is an unknown regression coefficient and $\bar{W}$ is the mean of all used values of $W(T)$.

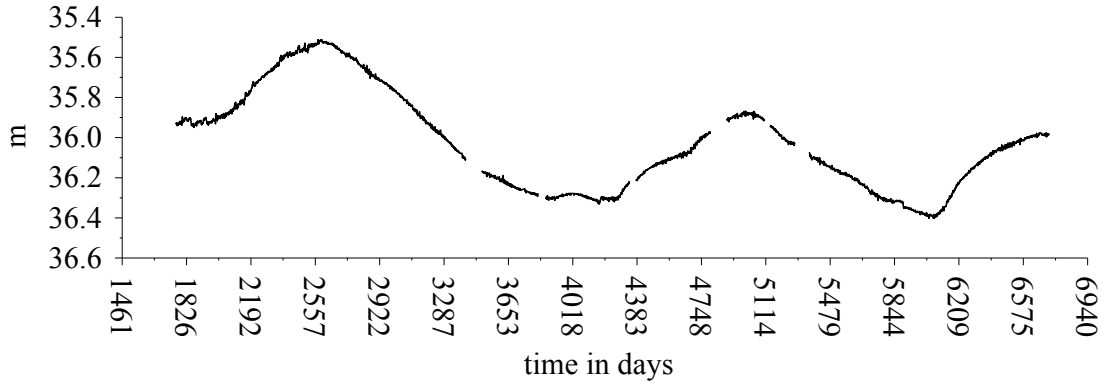


**Figure 11.** Observed variations $W(T)$ of the water table (descending vertical scale).

Unlike the other $\Delta G$ constituents of (8), $W(T)$ is a slowly varying function without clearly manifested periodic components. Due to this there appeared problems to use in parallel $W(T)$ in parallel with the polynomial model of $D_{\mathrm{ID}}$.

The use of (11) and $D_{\mathrm{ID}}$ represented by polynomials of power $k =$ , as shown in section 5.2, has given

$\delta_{\mathrm{pole}} =$ $\pm$ and $c_{\mathrm{WT}} =$ $\pm$ $^2$/m. (12)

This value of $\delta_{\mathrm{pole}}$ is not so bad, although it has a lower precision than the final value obtained without $\Delta G_{\mathrm{WT}}$ (Table 4 in Part 6). Much more disastrous is the estimated $c_{\mathrm{WT}}$, being a completely abnormal quantity - positive instead of negative, with extremely low precision.

Due to this the use of $W(T)$ as a tool for finding the estimate of $\delta_{\mathrm{pole}}$ has been abandoned Instead, we have attempted finding a reasonable estimate of $c_{\mathrm{WT}}$ by simplifying the use of the polynomials. After a series of experiments, it appeared reasonable to use the same points of discontinuities as in section 5.2, but decrease the power of the polynomials to $k =$ . The other two phenomena, temperature and annual component, remained in use as above.

The analysis in such a way has provided

$c_{\mathrm{WT}} =$ $\pm$ /m (13)

This value is in reasonable agreement with Delcout-Honorez (1991), who obtained $c_{\mathrm{WT}} = -28\ \mathrm{nms}^{-2}/\mathrm{m}$. In the same time, we have got $\delta_{\mathrm{pole}} =$ $\pm$ , which is obviously not satisfying.

### 5.6. Effect of the polar motion.

The theoretical model of $\Delta G_{\mathrm{pole}}$ for static deformation has been given by the expression (3). It implies that the theoretical effect $\Delta g_{\mathrm{pole}}$ on an absolute rigid (non-deformable) Earth and the observed effect $\Delta G_{\mathrm{pole}}$ on the real Earth are in phase.

One way to study the phase difference is to use a decomposition of $\Delta G_{\text{pole}}$ in series of periodic constituents (Loyer et al., 1999), with frequencies known from the study of the polar motion. Then we obtain the $\delta_{\text{pole}}$ factor (actually factors) in the frequency domain.

We preferred to remain entirely in the time domain. The real spectral structure of the polar motion is complicated and the frequencies are not very clearly defined. E.g., in the ancient data of Vondrak, one can find a double peak at the Chandler period.

For that reason the phase problem has been solved by using, instead of (3), the model

$$\Delta G_{\text{pole}}(T) = \delta_{\text{pole}} \Delta g_{\text{pole}}(T - \tau_{\text{pole}}) \qquad (14)$$

with time lag of the effect $\tau_{\text{pole}}$, positive for retardation.

In this model $\tau_{\text{pole}}$ is a parameter of the model, which should be estimated through its variation. Figure 12 shows the result from the experiments. The minimum of $\sigma(\delta_{\text{pole}})$, as well as the minimum of AIC happened at $\tau_{\text{pole}} = -96$ hours = -4 days, i.e. for an advance of the effect with 4 days.

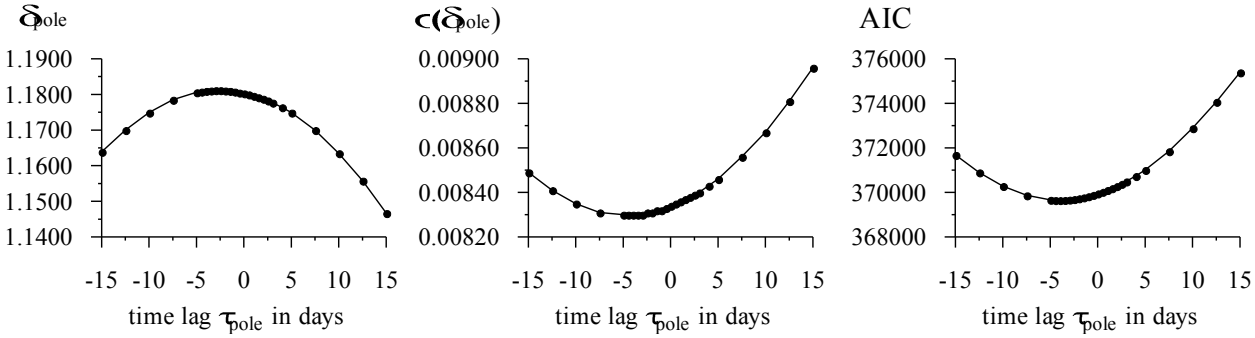


**Figure 12.** Estimated $\delta_{\text{pole}}$, its MSD $\sigma(\delta_{\text{pole}})$ and AIC as functions of the time lag $\tau_{\text{pole}}$ (positive for retardation).

In the same time, as shown in Table 3, the differences between the results for $\tau_{\text{pole}} = 0$ hours and $\tau_{\text{pole}} = -6^{\text{h}}$ are extremely small. So that the results $\tau_{\text{pole}} = 0^{\text{h}}$ and $\tau_{\text{pole}} = -6$ hours cannot be accepted as significantly different quantities. By the way, for the Chandler period the quantity $\tau_{\text{pole}} = -6^{\text{h}}$ corresponds to a phase advance of only 3°.35.

**Table 3.** Effect of the time lag $\tau_{\text{pole}} = -6^{\text{h}}$.

| $\tau_{\text{pole}}$ (hours) | $\delta_{\text{pole}}$ | $\sigma(\delta_{\text{pole}})$ | AIC |
|---|---|---|---|
| -96 | 1.1810 | 0.00830 | 369653 |
| 0 | 1.1803 | 0.00834 | 369955 |

The observed $\delta_{\text{pole}}$ value is much too large compared with the theoretical models, e.g. the DDW99 model for a non hydrostatic anelastic Earth model. However Boy & al. (2000) computed an amplitude factor $\delta_{\text{pole}} = 1.19$ taking into account the oceanic loading at the Chandler period. The phase advance too, which seems indeed not accurately determined, could also be explained by the oceanic loading.

## 7. FINAL RESULTS

Table 4 is a summary of our results.

**Table 4**. Final results.

| Component | Parameter | Numerical estimates | unit |
|---|---|---|---|
| Pole tide | $\delta_{pole}$ | **1.1810 ± 0.0083** | |
| | $\tau_{pole}$ | **-96 (advance)** | hours |
| Annual components (only amplitudes of the first harmonics) | (1 cpy) | 39.05 ±0.52 | $nms^{-2}$ |
| | (2 cpy) | 5.10 ±0.34 | $nms^{-2}$ |
| Temperature | $c_{temper}$ | -1.735 ±0.047 | $nms^{-2}/^{o}C$ |
| | $\tau_{temper}$ | 52 (retardation) | hours |
| Water table | $c_{WT}$ | -149.54 ±2.75 | $nms^{-2}/m$ |

Figure 13 is a graphical illustration of the approximation process.

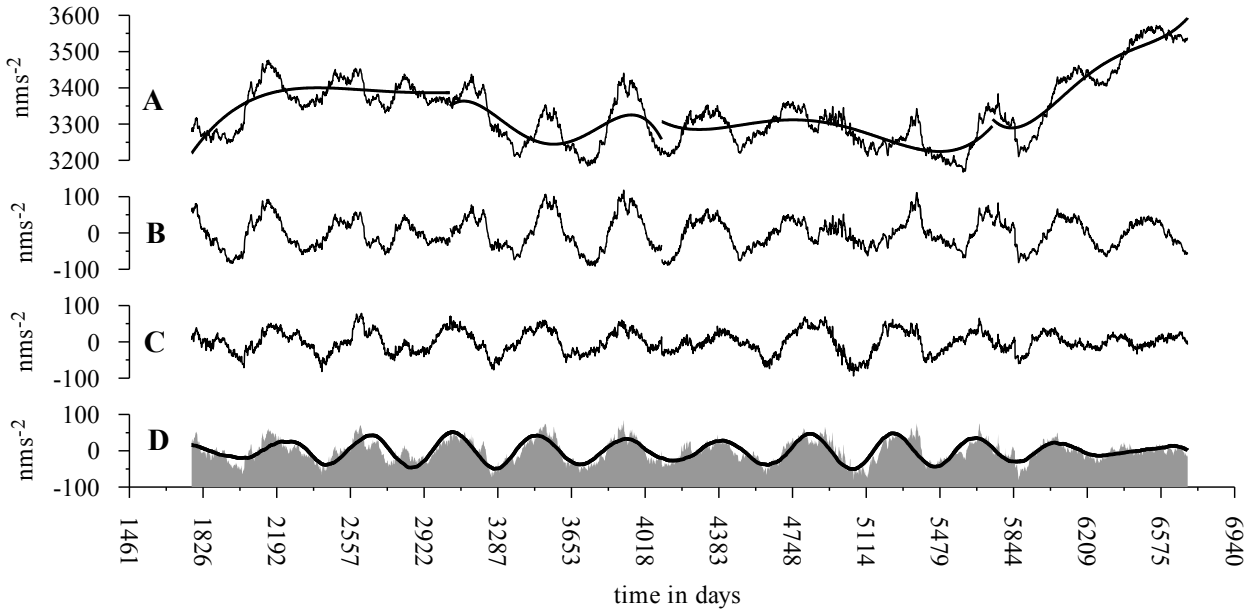


**Figure 13.** (A) Estimated drift $d_0(T)$ & polynomial approximation of the instrumental drift $D_{\mathrm{ID}}(T)$ in 4 blocks, (B) $d_0(T)$ reduced by the approximation of the instrumental drift, (C)

$d_0(T)$ reduced by the approximation of the instrumental drift as well as by the effects of the annual and the temperature components and (D) estimated effect of the polar motion $\Delta_{\text{pole}}G(T) = \delta_{\text{pole}}\Delta g_{\text{pole}}(T - \tau_{\text{pole}})$ (bold line), compared with the observed effect in (C) (the filed grey curve).

## 7. CONCLUSIONS

From a 13½ years observation period performed in Brussels with the GWR T003 Superconducting Gravimeter we tried to determine the amplitude factor $\delta_{\text{pole}}$ of the pole tide by modeling the effect of different perturbing factors. We used the VAV/2002 program to evaluate simultaneously in the signal the tidal part and the non tidal one, often referred as "drift", as well as residual gravity. The spectral content of this drift signal shows beside the polar motion effect, strong annual and semi-annual oscillations, as well as aperiodic fluctuations. As auxiliary signals we can use pressure, temperature and water table variations. The aperiodic fluctuations in the drift are partly explained by the water table with a coefficient $\delta_{\text{pole}}$ close to -150nms$^{-2}$/m. However the aperiodic signal includes jumps and it was necessary to use a polynomial representation though a partition of the data in 4 blocks. The temperature signal is explaining only a part of the annual gravity signals and it was necessary to introduce an a priori annual wave and its harmonics of higher order. To find the optimal adjustment we tried to minimize the RMS error or MSD on the $\delta_{\text{pole}}$ factor as well as the AIC criterion. The best estimated value seems to be $\delta_{\text{pole}} = 1.1810 \pm 0.0083$. This large increase of the tidal amplitude factor at periods close to one year with respect to recent models of the Earth response including inelasticity in the mantle is essentially due to the ocean pole tide. It will be necessary to compute an ocean loading correction based on the modeled ocean pole tide by Desai (2002).

It is obvious that the stacking of different superconducting gravimeter data from various stations could produce a more robust evaluation of $\delta_{\text{pole}}$ as the perturbations will not build up unlike the pole tide signal. As we have now some series close to 10 years a composite solution is already possible.

## ACKNOWLEDGMENTS

The authors wish to thank all the Observatory staff members who took part to the installation and the maintenance of the superconducting gravimeter as well as to the data acquisition and reduction: J. Barthélemy, M. Hendrickx, R. Laurent, C. Poitevin, F. Renders, A.Somerhausen, L. Vandercoilden, T. Van Hoolst, A. Vandewinkel.

P.Melchior and P.Pâquet always supported this work as directors of the Royal Observatory of Belgium.

R. Warburton performed himself the first installation and provided solutions to all the technical problems.

One of the authors (A. Venedikov) has been supported by the State Secretariat for Education and Universities at the Spanish Ministry of Education and Culture. Projects REN2002-0054/RIES and REN2001-2271/RIES of Spanish Ministry of Science and Technology have also supported this work.

## REFERENCES

Boy J.P., Hinderer J., Amalvict M., Calais E., 2000. On the use of long records of superconducting and absolute gravity observations with special application to the Strasbourg station, France.Cahiers du Centre Européen de Géodynamique et de Séismologie, 17, 67-83

Crossley, D., Hinderer, J., Casula G., Francis O., Hsu, H.T., Imanishi, Y., Jentzsch G., Kääriäinen J., Merriam, J., Meurers B., Neumeyer J., Richter B., Shibuya K., Sato T., Van Dam T., 1999. Network of superconducting gravimeters benefits a number of disciplines. EOS, 80, 11, 121-126.

Dehant, V., Defraigne, P. and Wahr, J., 1999. Tides for a convective Earth. J. Geophys. Res., 104, B1, 1035-1058.

Delcourt-Honorez, M., 1991. Water-levels fluctuations in a borehole at the Royal Observatory of Belgium: effects on local gravity, earth tidal and barometric responses. In: Juhani Kakkuri (Editor). Proc. 11th Int. Symp. on Earth Tides, Helsinki, July 31-August 5, 1989, E. Schweizerbart'sche Verlagsbuchhandlung, Stuttgart, 389-412.

De Meyer F., Ducarme B., 1991. Non tidal gravity changes observed with a superconducting gravimeter. In: Juhani Kakkuri (Editor). Proc. 11th Int. Symp. on Earth Tides, Helsinki, July 31-August 5, 1989, E. Schweizerbartsche Verlagsbuchhandlung, Stuttgart, 167-184

Desai S.D. (2002). Observing the pole tide with satellite altimetry. J. Geophys. Res., 107, C11, 3186, doi:10.1029/2001JC001224.

Francis O.,Ducarme B., De Meyer F., Mäkinen J., 1995. Present state of absolute gravity measurements in Brussels and comparison with the superconducting gravimeter drift. Cahiers Cent. Europ. Géod. Séismol., 11, 117-123

Melchior, P., 1983. The tides of the planet Earth. 2nd Edition, Pergamon Press, Oxford, 641 pp.

Sakamoto, Y., Ishiguro, M., Kitagawa, G., 1986. Akaike information criterion statistics, D. Reidel Publishing Company, Tokyo, 290 pp.

Tamura, Y., 1987. A harmonic development of the tide-generating potential. Bull. Inf. Marées Terrestres, 99, 6813-6855.

van Ruymbeke, M., Delcourt-Honorez, M., 1986. A capacitive transducer for water-level measurements: "Nivocap". In: Ricardo Vieira (Editor). Proc. 10th Int. Symp. on Earth Tides, Madrid, September 23-27, 1985, Consejo Superior de Investigaciones Científicas, 95-102.

Venedikov, A.P., Arnoso, J., Vieira, R., 2001. Program VAV/2000 for tidal analysis of unequally spaced data with irregular drift and colored noise. J. Geodet. Soc. Japan, 47, 1, 281-286.

Venedikov, A.P., Arnoso, J., Vieira, R., 2003. VAV: a program for tidal data processing. Comp. and Geosc. (in press)

Wenzel, H.G., 1996. The nanogal software: data processing package ETERNA 3.3. Bull. Inf. Marées Terrestres, 124, 9425-9439.